IL NUOVO CIMENTO **47 C** (2024) 121
DOI 10.1393/ncc/i2024-24121-1

Colloquia: IFAE 2023

Energy threshold calibration of the GAPS experiment Si(Li) tracker readout electronics(*)

L. Ghislotti(1)(2)(**), M. Boezio(3), L. Fabris(4), P. Lazzaroni(2), M. Manghisoni(1)(2), L. Ratti(5), V. Re(1)(2), E. Riceputi(1)(2) and G. Zampa(3)

(1) *Department of Engineering and Applied Sciences, University of Bergamo - Dalmine, Italy*
(2) *INFN, Pavia Section - Pavia, Italy*
(3) *INFN, Trieste Section - Trieste, Italy*
(4) *Oak Ridge National Laboratory - Oak Ridge, TN, USA*
(5) *Department of Electrical, Computer and Biomedical Engineering, University of Pavia Pavia, Italy*

received 13 February 2024

Summary. — GAPS (General AntiParticle Spectrometer) is a stratospheric balloon experiment designed to detect low-energy cosmic ray antinuclei (< 0.25 GeV) as an indirect signature of dark matter. The experiment exploits an innovative particle identification approach based on the formation of an excited atom and its consequent de-excitation and decay. GAPS will provide unprecedented sensitivity to cosmic antideuterons, an antiproton spectrum in a hitherto unexplored energy range and high sensitivity to cosmic antihelium. The first flight is foreseen to take place from the McMurdo Station in Antarctica during the austral summer of 2024. The instrument is currently undergoing integration and calibration in anticipation of launch. In this paper, the latest tracker electronics energy threshold calibration results will be presented.

1. – The instrument

The GAPS instrument consists of a Time-of-Flight (ToF) system composed of 160 plastic scintillators [1] surrounding a tracker composed, for the initial flight, of seven layers each containing 144 Lithium-drifted Silicon (Si(Li)) detectors [2]. The ToF provides the velocity measurement of the incoming antinuclei and serves as the trigger for the inner tracker electronics. Figure 1 (left) shows the GAPS instrument assembly, highlighting the Si(Li) tracker and the three components of the ToF system. The latter serves as a target for the particles of interest and X-ray spectrometer and is capable of measuring keV-MeV energies with a resolution of 4 keV in the 10–100 keV range. Si(Li) detector readout is performed by an Application Specific Integrated Circuit (ASIC) designed in

(*) IFAE 2023 - "Poster" session
(**) E-mail: luca.ghislotti@unibg.it

Creative Commons Attribution 4.0 License (https://creativecommons.org/licenses/by/4.0)

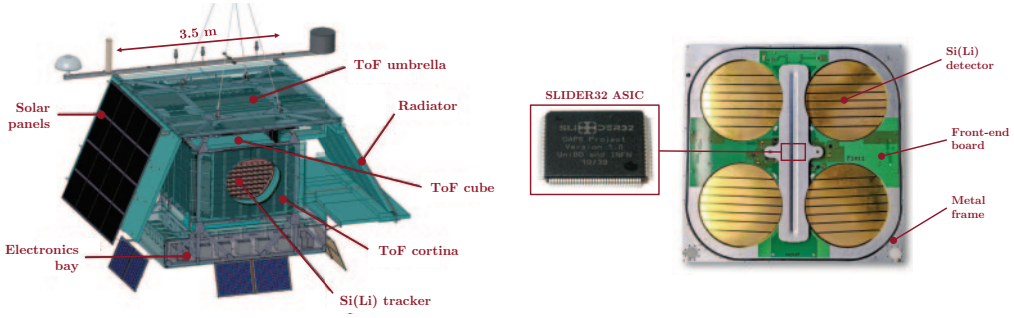

Fig. 1. – (Left) GAPS instrument assembly. Indicated are the Si(Li) tracker and the three components of the ToF system. (Right) GAPS Si(Li) tracker module.

180 nm CMOS technology [3]. A Si(Li) tracker module, shown on the right in fig. 1, includes a Front-End Board (FEB) that houses the readout ASIC [4] and allows the connection to four Si(Li) detectors, each subdivided into eight independent strips and maintained at a temperature of −40 °C by means of an innovative cooling system based on the principle of oscillating heat pipe [5] coupled to a radiator.

2. – Si(Li) tracker electronics

The Si(Li) detector readout chip, named SLIDER32 (32-channels SiLI DEtector Readout) consists of 32 low-noise analog readout channels to process signals coming from the Si(Li) detector strips, an 11-bit ADC (Analog-to-Digital Converter) and a digital backend [6]. The analog channel, whose simplified schematic is presented in fig. 2, includes a Charge Sensitive Amplifier (CSA) that employs a non-linear MOS capacitor in its feedback loop, featuring dynamic signal compression. This allows the CSA to cope with a wide input dynamic range from 20 keV to 100 MeV, while preserving good resolution at low energies. A Krummenacher network [7] is responsible for charge restoration in the feedback capacitance and for compensating the detector leakage current, measured to be less than 10 nA at −40 °C. The amplifier is followed by a unipolar second order semi-Gaussian filter with 8 selectable peaking times, in the 0.25–1.6 µs range. The sampling signal can be provided either from outside the ASIC, with an external trigger generated from the ToF system, or internally in self-trigger mode. The latter is implemented via an active differentiator followed by a zero-crossing circuit that provides a trigger, synchronous with the shaper peaking time, to a single-ended to differential Sample&Hold (S&H). This block provides an output signal proportional to the peak of the signal coming from the shaper.

3. – Calibration in self-trigger mode

During integration of the GAPS instrument, a calibration procedure was established to accurately reconstruct the self-trigger energy threshold of all Si(Li) tracker analog readout channels. The method enabled the estimation of Equivalent Noise Charge (ENC) for the channels, allowing a comparison with values obtained through pedestal measurements. This validation was conducted by evaluating the energy spectrum acquired using a ^{109}Cd source. Experimental threshold assessment has been performed during a charge-

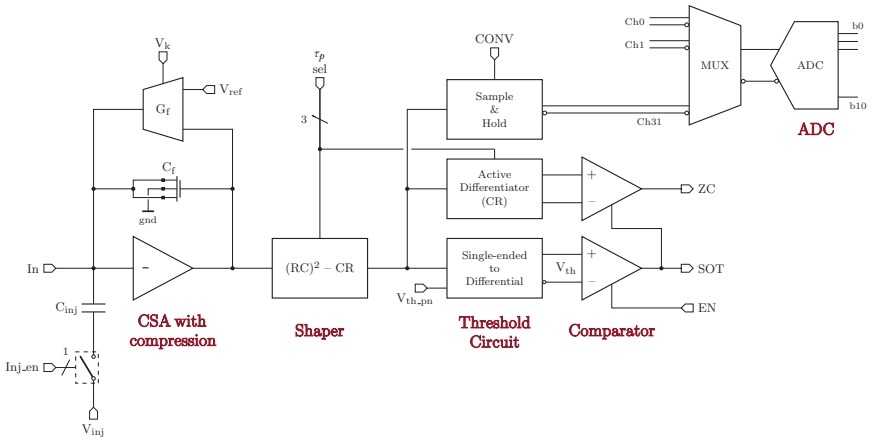

Fig. 2. – SLIDER32 analog readout channel schematic.

scan test by injecting an equivalent charge in the 1 keV ÷ 120 keV energy range with a dedicated charge injection circuit, included in each channel of the ASIC. The circuit consists of an injection capacitance and a commercial 16-bit DAC (Digital-to-Analog Converter) mounted on the FEB, providing a tunable injection voltage step. Each channel's digital output is read out by an FPGA (Field Programmable Gate Array) and a dedicated Data Acquisition System (DAQ). For a given threshold setting, the channel is injected a fixed number of times for each value in the considered range. The number of times the channel is triggered is then measured and plotted with respect to the corresponding energy value, as done on the left in fig. 3. The measurements are distributed as a normal random variable $X \sim \mathrm{Norm}(\mu, \sigma)$ with mean μ and standard deviation σ.

The channel's self-trigger energy threshold is calculated at 50 % trigger probability considering the normal distribution cumulative function $\Phi(x, \mu, \sigma)$ calculated using the error function $\mathrm{Erf}(x)$ with an additional normalization factor k to take into account the number of injections for each energy step. The channel energy threshold is represented

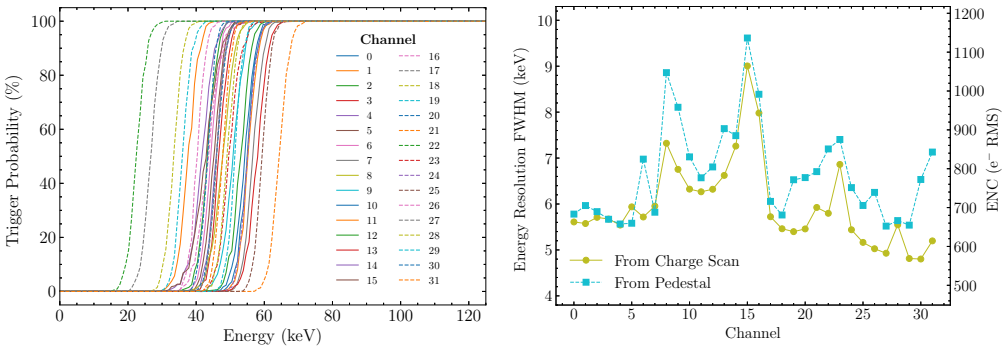

Fig. 3. – (Left) Charge scan of a tracker module with 50 keV threshold. (Right) ENC obtained from charge scan and pedestal of all channels of the same tracker module.

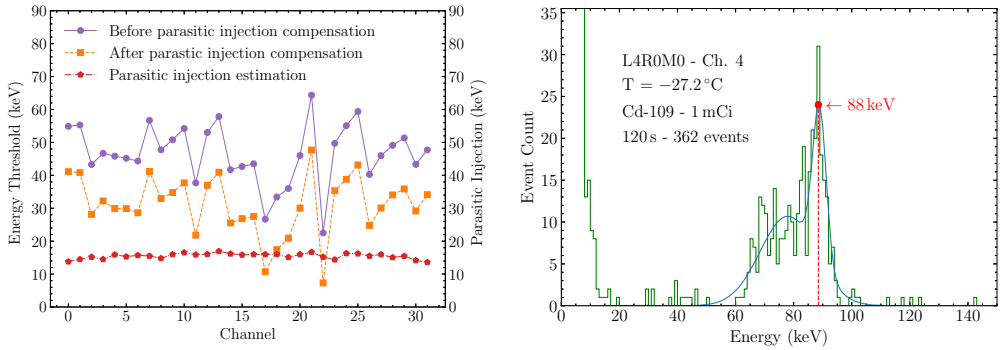

Fig. 4. – (Left) Thresholds of all channels of a tracker module before and after parasitic injection compensation obtained from charge scan. (Right) ^{109}Cd 88 keV X-ray peak acquired on channel 4 of the same tracker module.

by the mean value μ, while the standard deviation σ is the ENC at the channel input, as reported in the following equation:

$$\Phi(x, \mu, \sigma, k) = \frac{1}{2} k \left[1 + \mathrm{Erf}\left(\frac{x - \mu}{\sigma\sqrt{2}} \right) \right]. \tag{1}$$

ENC estimation has been validated considering the electronic noise as the root-mean-square (rms) of the voltage fluctuations of the analog channel pedestal and calculating it as the standard deviation of the channel pedestal divided by its gain. The comparison is reported on the right in fig. 3. Noise measurements are consistent, albeit in excess of the expected value of 4 keV. This is attributed to the suboptimal measurement conditions, not comparable to those expected in flight. During on-ground calibration, the Si(Li) tracker is kept cool via an auxiliary cooling system, which is unable to guarantee the detector's operating temperature of −40 °C, leading to a larger detector leakage current and a higher parallel noise contribution. The measured temperature of the module in question is −27.2 °C. Thresholds obtained from charge scan analysis are reported on the left of fig. 4 before and after parasitic injection compensation. This refers to the evaluation of the additional capacitance of the injection circuit that causes an additional charge injection at each energy step. Parasitic injection has been estimated by comparing the channel pedestal to the one calculated considering the intercept of a linear model fit of the channel transfer function in the 10–120 keV energy range. This procedure allowed to determine the real channel energy threshold by subtracting the parasitic injection contribution to the threshold obtained during the charge scan.

Threshold dispersion has been minimized by adjusting the channel threshold via a 3-bit fine threshold DAC around its global threshold setting, determined by an 8-bit DAC that acts on all 32 channels of a module. On a total of 9920 channels (310 ASICs) the initial 25.3 keV threshold dispersion has been reduced to 14.3 keV, with a 43 % overall improvement. To validate the calibration procedure, a ^{109}Cd source has been used. On the right of fig. 4, the energy spectrum of a self-triggered acquisition on a single channel is presented, where the 88 keV X-ray peak is visible. The lower energy tail is associated with events truncated at the edge of a strip, for which part of the energy is lost on

adjacent strips. The lower limit is provided by the channel energy threshold, that for channel 4 is 45.8 keV before parasitic injection compensation and 29.9 keV thereafter. The evaluated energy resolution is 5.5 keV and is consistent with the previously stated noise measurements for channel 4.

4. – Conclusions

In this paper, the GAPS Si(Li) tracker energy threshold calibration procedure was presented. The calibration activity enabled the self-trigger energy threshold of all Si(Li) tracker analog readout channels to be determined, allowing low-threshold channels to be identified and deactivated. ENC measurements from charge scans are consistent with those obtained from pedestal and ^{109}Cd energy spectrum acquisition. The reported results paved the way for several further validation and calibration activities, currently in progress in anticipation of the launch.

REFERENCES

[1] Feldman S. N., *PoS*, **ICRC2023** (2023) 120.
[2] Xiao M. *et al.*, *Nucl. Instrum. Methods Phys. Res.*, **1034** (2022) 166820.
[3] Re V. *et al.*, *Nucl. Instrum. Methods Phys. Res.*, **1045** (2023) 167617.
[4] Riceputi E. *et al.*, in *Proceedings of SIE 2022, Pizzo (Italy), 7–9 September 2022*, Vol. **1005** (Springer, Cham) 2023.
[5] Okazaki S. *et al.*, *Appl. Therm. Eng.*, **141** (2018) 20.
[6] Manghisoni M. *et al.*, *IEEE Trans. Nucl. Sci.*, **68** (2021) 2661.
[7] Krummenacher F., *Nucl. Instrum. Methods Phys. Res.*, **305** (1991) 527.